A R C H I V E S O F M E T A L L U R G Y A N D M A T E R I A L S
Volume 53 2008 Issue 1

J. KOWALSKA* , W. RATUSZEK*, K. CHRUŚCIEL*

CRYSTALLOGRAPHIC RELATIONS BETWEEN DEFORMATION AND ANNEALING TEXTURE IN AUSTENITIC STEELS

RELACJE KRYSTALOGRAFICZNE POMIĘDZY TEKSTURĄ ODKSZTAŁCENIA I WYŻARZANIA W STALACH AUSTENITYCZNYCH

Orientation relationships between deformation and annealing textures of chromium-nickel austenitic stainless steel have been analysed in the present paper. Two austenitic steels of different chemical compositions and phase stability were investigated after deformation and annealing i.e. the X7CrNi24-11 and X10CrNi18-7. Since both steels exhibited stable and metastable austenite structure a different deformation and annealing textures were obtained in each of them as a consequence.

The texture of austenite after deformation of both steels showed the brass type texture {110}<112>. The appearances of the {111}<uvw> components in both textures resulted from mechanical twinning.

The texture of the α′-martensite formed in the metastable steel during deformation became stronger with increasing deformation degree. The orientation relationships between the major austenite and martensite textures components were best described by K u r d j u m o v-S a c h s orientation relationship.

The appearance of new orientations in the austenite texture was observed after annealing of the stable steel, apart from the weakening of main texture component. In order to determine crystallographic relations between deformation and annealing textures, the transformation of ideal orientations as well as experimental orientation distribution functions (ODFs) was carried out without variant selection. It was found that twin relation, (that is the 60° <111> rotation) described these relationships in an appropriate way. However, the process of oriented growth might have also affected also the annealing textures of austenite to some extent.

Crystallographic relations between the orientations from the annealing texture of austenite and the deformation texture of martensite in the metastable steel followed best the K u r d j u m o v-S a c h s relationship. Additionally, some texture relations of the deformed and annealed austenite were described by a twin relationship. The orientations describing texture of annealed austenite resulted from both, the inverse transformation (α′ → γ) and the recrystallisation of deformed austenite.

Keywords: austenitic steel, deformation, annealing, texture, transformation, crystallographic relation, orientation distribution functions (ODF)

W pracy analizowano relacje krystalograficzne pomiędzy teksturą odkształcenia i wyżarzania nierdzewnych stali austenitycznych chromowo-niklowych. Przebadano dwie stale austenityczne różniące się składem chemicznym i stabilnością fazową: stabilną stal X7CrNi24-11 i metastabilną stal X10CrNi18-7.

W obu stalach tekstura austenitu po odkształceniu dążyła do tekstury typu stopu {110}<112>. Obecność składowej {111}<uvw> świadczyła o pewnym udziale mechanicznego bliźniakowania w tworzeniu tekstury.

W stali metastabilnej podczas odkształcania powstawał martenzyt którego tekstura ulegała wzmocnieniu wraz ze wzrostem deformacji. Zależności krystalograficzne pomiędzy teksturą austenitu i teksturą martenzytu powstałego w wyniku odkształcenia najlepiej opisywała relacja K u r d j u m o w a-S a c h s a.

Wyżarzanie stali stabilnej doprowadziło do osłabienia głównych składowych tekstury odkształcenia i pojawienia się nowych orientacji w teksturze austenitu. W celu określenia zależności krystalograficznych pomiędzy teksturą odkształcenia i wyżarzania przeprowadzono transformację idealnych orientacji jak również eksperymentalnych funkcji rozkładu orientacji bez selekcji wariantów. Stwierdzono że obrót o 60° <111> – relacja bliźniacza opisuje te zależności. Na tekstury wyżarzania austenitu wywierają również wpływ relacje opisane zorientowanym wzrostem.

Zależności krystalograficzne pomiędzy orientacjami występującymi w teksturze wyżarzania austenitu i teksturze odkształcenia martenzytu stali metastabilnej najlepiej opisuje relacja Kurdjumowa-Sachsa. Pochodzenie niektórych orientacji występujących w teksturze austenitu odkształconego i wyżarzonego można wyjaśnić relacją bliźniaczą. Orientacje opisujące teksturę austenitu wyżarzonego są efektem zarówno zajścia przemiany odwrotnej α′ → γ, jak i rekrystalizacji austenitu odkształconego.

* DEPARTMENT OF PHYSICAL AND POWDER METALLURGY, AGH – UNIVERSITY OF SCIENCE AND TECHNOLOGY, 30-059 KRAKÓW, AV. MICKIEWICZA 30, POLAND

1. Introduction

The phase transformations as well as the crystallographic relationships between austenite and the products of the transformation like ferrite, bainite or martensite, play an important role in commercial Fe based alloys. They were subjects of numerous investigations [1–16].

In the phase transformation which proceeds according to a special crystallographic relation, a single original orientation changes into a number of final crystallographic orientations depending on the symmetry and the initial orientation of the crystal. From the crystallographic point of view, all possible variants resulting from the transformation should appear with the same probability. However, strong differentiation of the probability of some variants has been observed in practice. The crystallographic relationships that are most often observed in steels are Bain, Kurdjumov-Sachs (K-S) and Nishiyama-Wassermann (N-W) [16].

On the other hand the formation of the recrystallisation textures is connected with to the appearance and growth of nuclei [17–20]. Essentially there are two theories of recrystallisation texture formation: theory of oriented growth and theory of oriented nucleation.

2. Material and experimental procedure

The experiments were carried out on two stainless chromium-nickel steels of different composition and phase stability (Table 1). The X7CrNi24-11 steel was produced in the laboratory conditions. The ingot was homogenized and then hot forged at 900–1000°C. The obtained rods were annealed at 1050°C for 3 hrs and water cooled and subsequently cold rolled up to 80% of reduction. The annealing was conducted within the temperature range 750–1000°C for 1 hour.

The X10CrNi18-7 steel was the industrially production. It was hot rolled and solution treated and then cold rolled to obtain 88% of deformation and annealed at various temperatures from the range of 550–950°C for 1 hour.

Based on the compositions of both steels, the R_{Cr} and R_{Ni} equivalents, stacking fault energy (SFE), the martensitic start temperature (Ms) and temperature of martensitic transformation induced by deformation ($M_{D30/50}$) were calculated (Table 2) [12–14].

The diffraction investigations were performed by means of Bruker D8 Advance Diffractometer using Co Kα radiation of $\lambda_{K\alpha}$ = 1.79Å. In texture measurements pole figures, three for each of {111}, {200}, {220} planes in austenite and for {110}, {200} and {211} planes of martensite were recorded. The measurements were carried out in the central part of the sheets.

3. Results

The austenite in the initial state displayed very weak texture (Fig. 1). In the X7CrNi24-11 (with stable austenite) the texture after 80% deformation could be described by a limited fibre α =<110>|| ND, as well as weak
orientations belonging to the γ = {111}<uvw> fibre. The strongest texture component of deformed austenite was ~{110}<113> with the maximum value of ODF = 5.4. Additionally, the {738}<151> orientation (shown in section φ_2 = 65°) (Fig. 2) was also observed within the austenite texture.

TABLE 1

The chemical compositions of the austenitic steels

Chemical compositions of steels [wt. %]												
Steel	C	Cr	Ni	Mn	Mo	Si	Cu	Ti	V	Nb	N_2	Fe
Stable	0.07	23.91	11.09	0.20	0.089	0.30	0.058	0.019	0.074	–	0.066	balance
Metastable	0.1	17.6	7.48	1.08	0.114	0.6	0.14	<0.005	–	<0.005	0.077	balance

TABLE 2

Properties of the austenitic steels

Steel	R_{Cr}	R_{Ni}	EBU [mJ/m^2]	M_s [°C]	$M_{D30/50}$ [°C]
Stable	~25	~13.3	33.9	−177.5	−90
Metastable	~19	~13	10.21	−131	8.13

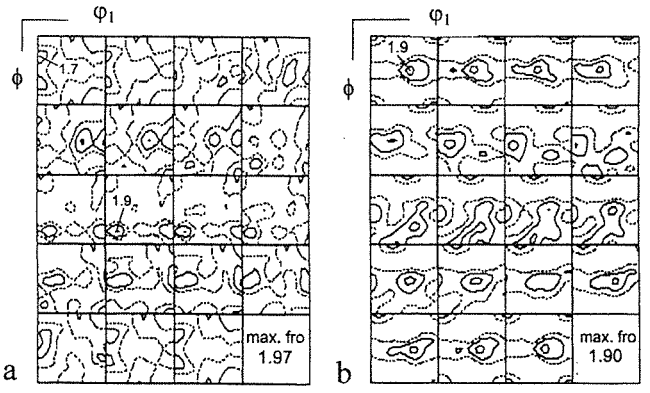

Fig. 1. Orientation distribution functions (ODF) for the materials in the starting stage: (a) of austenite for the stable X7CrNi24-11 steel, (b) the metastable X10CrNi18-7 steel

The development of the deformation texture in the metastable steel was complex, because, the texturization of the austenite, martensitic $\gamma \rightarrow \alpha'$ transformation (in which relationship between them γ and α' phases was preserved), as well as the change of the martensite orientation formed at deformation took place simultaneously. The components of the both, austenite and martensite thus described the deformation texture of the metastable steel.

The austenite of the metastable steel after 88% deformation had a sharp texture. It could be described by a sharp α = <110>||ND fibre with maximum value of ODF = 8.5, which corresponded to the {110}<229> orientation, while the remaining weak ones corresponded to {125}<358> and {113}<332> orientations (Fig. 3). The presence of the {111}<uvw> component in the texture of austenite suggested a contribution of mechanical twinning in the formation of the texture. The orientations of the α_1 = <110>||RD fibre prevailed in the texture of the 88% deformed martensite. Maximum value of ODF corresponded to the {111}<112> orientation (Fig. 3).

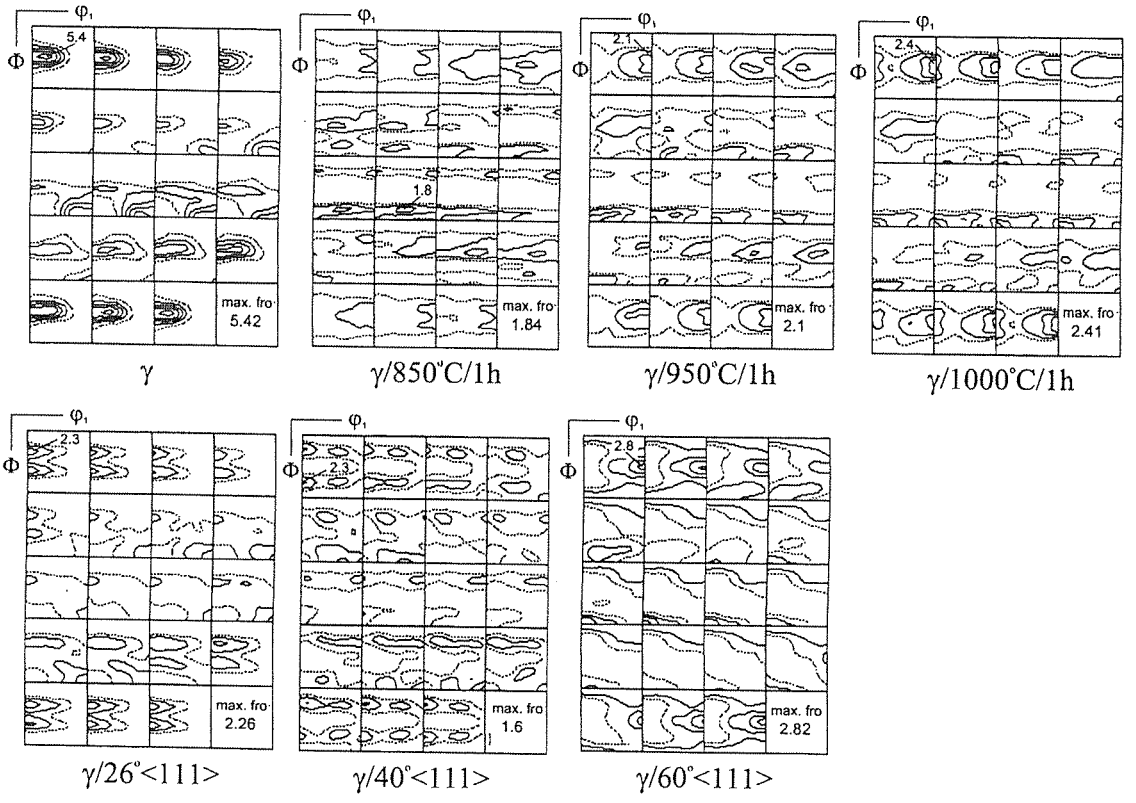

Fig. 2. Orientation distribution functions (ODF) of austenite deformed up to 80%, after annealing and rotated bu the angles 26, 40 and 60° around <111> poles for the stable X7CrNi24-11 steel

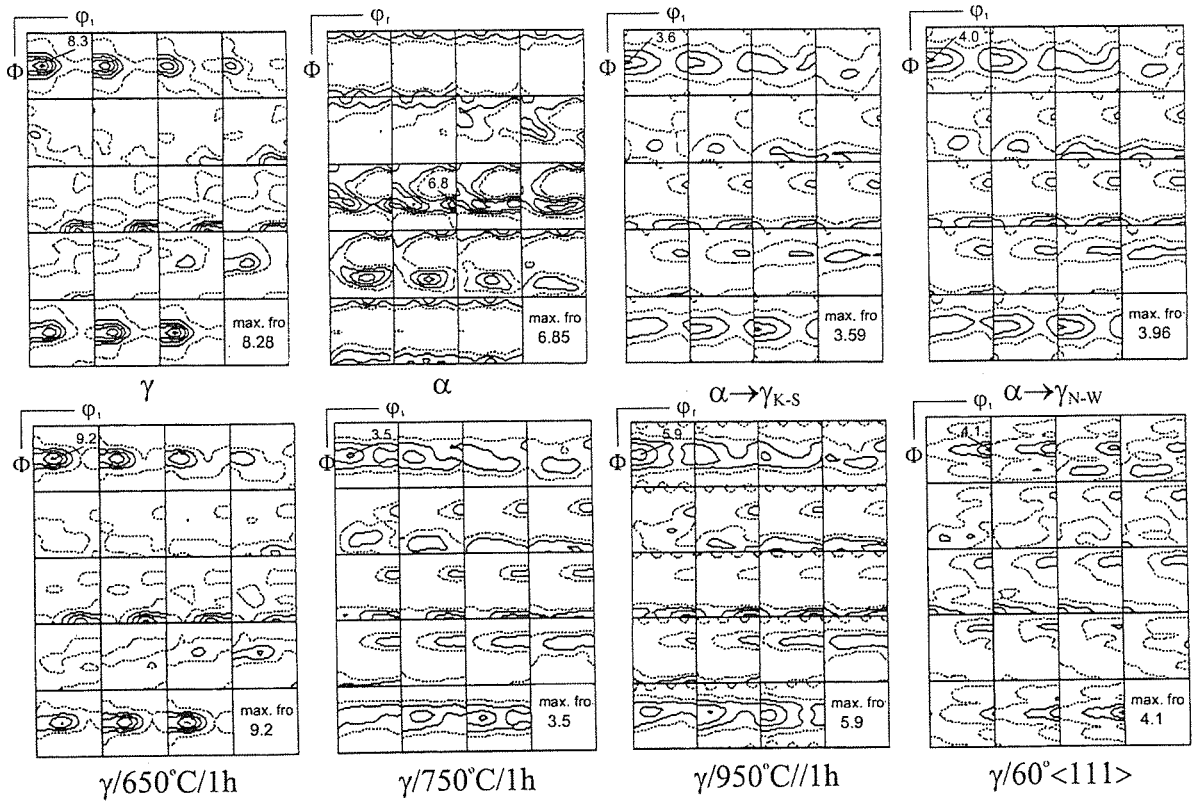

Fig. 3. Orientation distribution functions (ODF) of austenite (γ) and martensite (α) after 88% deformation, after α → γ transformation according to Kurdjumov-Sachs (K-S) and Nishyama-Wassermann (N-W), 88% deformed and annealed austenite and rotated by 60° angle around <111> poles for the metastable X10CrNi18-7 steel

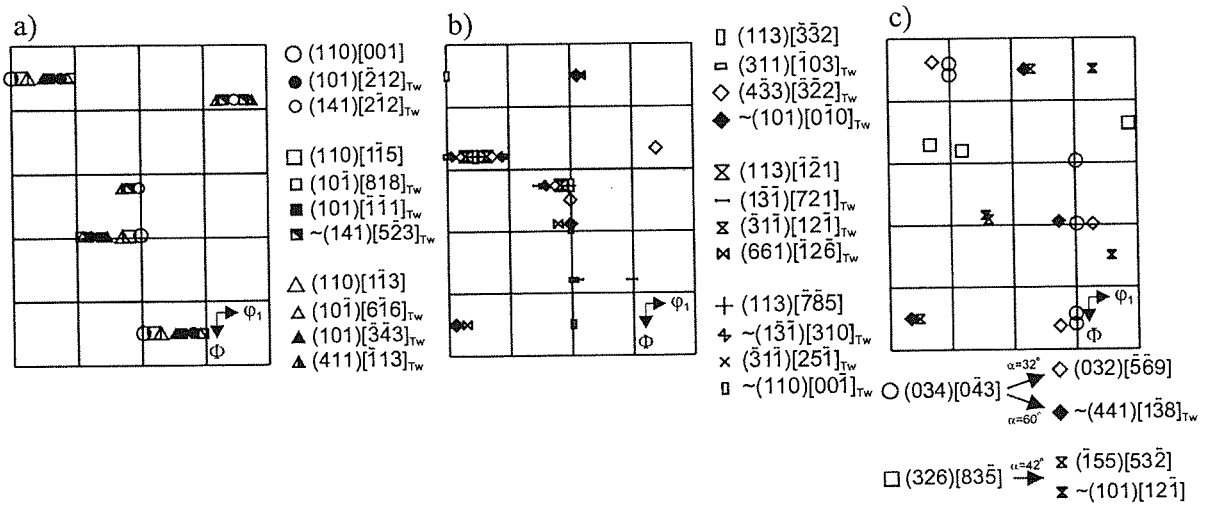

Fig. 4. Transformation of the ideal {110}<uvw> orientations (α-fibre) in the rolling texture (a), transformation of the {113}<uvw> orientations in the recrystallization texture according to twin relation (b), transformation (034)[043] and (326)[835] in the austenite recrystallization texture according to 32–60°<111> rotations (c) (section φ_2 = const)

The comparison of the ODF of austenite after deformation with the ODF obtained through the $\alpha' \rightarrow \gamma_T$ transformation conducted without variant selection confirmed, that the Kurdjumov-Sachs as well as Nishiyama-Wasserman relationships described well the crystallographic relations of austenite and martensite (Fig. 3). The differences in ODFs of the austenite obtained as the result of deformation and after the $\alpha' \rightarrow \gamma_T$ transition resulted from the fact, that the transformation referred to the orientation distribution of the martensite already deformed and martensite arising at a given deformation stage.

When comparing the deformation texture of austenite in the stable and metastable steel it could be noticed that in both materials the texture of austenite was close to the {110}<112> alloy-type texture. The martensite, which appeared in the metastable steel due to deformation, was strongly textured. On the other hand in the stable steel with a small amount of ferrite, the observed texture of the second phase was weak, due to its small amount.

The annealing at 750°C/1h resulted in texture changes of the stable steel. The α = <110>||ND fibre became diffuse and spread. The ODF maximum corresponded to the ~{277}<764> orientation. The decrease of ODF value for the Goss {110}<001> and {110}<112> orientations was observed and the fibre of the γ = {111}<uvw> orientation decayed. Weak orientations, such as {113}<332> and {326}<385> appeared in the texture (Fig. 2). The maximum value of ODF after the annealing at 800°C/1h corresponded to the {110}<110> orientation, while the {110}<001> and {110}<112> ones weakened. The α = <110>||ND fibre was separated in its final part into {034}<043> components (Fig 2). The increase of annealing temperature up to 950°C and 1000°C shifted the ODF maximum to the {034}<043> orientation. Apart from the already existing {113}<332> and {326}<385> orientations, new ones appeared as the components of fibre ε = <001>||RD {034}<001> (ODF = 1.7) (Fig. 2).

3.1. Orientation Relations between Textures

In order to carry out a full analysis of the relations between the deformation and annealing textures of the austenite in the stable steel, the transformation of ideal orientations as well as experimental ODF was performed without selection (Fig. 2 and 4). It was found out, that the twin relation reflected very well the crystallographic relationships between the deformation and annealing textures of austenite. However, some texture components could be still described according to the theory of oriented growth assuming the rotation around the common <111> pole as can be seen in Fig. 2 and 4.

The annealing of the metastable steel at 550°C did not cause the change of the type of austenite texture. Slight differences were visible in the maximum ODF values. The austenite texture after deformation referred to the {110}<229> orientation at maximum ODF = 8.2, then the maximum shifted to the {110}<113> as a result of annealing (Fig. 3). The martensite texture did not reveal any changes either.

The sharpening of the texture was observed in the texture of austenite after annealing at 650°C as a result of the occurrence of intensive reverse transformation phases $\alpha' \rightarrow \gamma$. However, the {110}<113> orientation remained the strongest component in the α = <110>||ND fibre. Apart from it, a weak diffuse {123}<364> orientation was also seen (Fig. 3). The martensite texture also showed significant changes after the annealing. The intensity of texture decreased and changes were detected in the α_1 = <110>||RD fibre in which the strongest component after deformation was the {111}<110> orientation. The annealing shifted the intensity maximum in the α_1 fibre towards {001}<110>, which became the strongest component of the martensite texture at that stage of heat treatment (Fig. 3).

After annealing at the temperature 750°C, the weakening of the austenite texture was registered. The α = <110>||ND fibre has undergone spreading and the diffuse {123}<356> and {113}<332> orientations appeared at this temperature with the {112}<111> orientation of Cu-type within the spread of the last one (Fig. 3). Annealing of this temperature resulted in the complete $\alpha' \rightarrow \gamma$ reverse transformation and that is why, martensite no longer existed in the annealed sample. The increase of temperature up to 850°C resulted in further texture changes. The α = <110>||ND fibre became spread, the strongest component the {110}<112> orientation. Apart from it, the appearance of the {113}<332> and {123}<364> orientations was found in the texture (Fig. 3). After the annealing at 950°C the appearance of additional components of the austenite texture such as {034}<100> was observed (Fig. 3).

The annealing texture of the austenite in the metastable steel consisted of textures of the deformed austenite and those of austenite formed due to the $\alpha' \rightarrow \gamma$ reverse transformation. With increasing temperature of annealing and proceeding of the $\alpha' \rightarrow \gamma$ transformation, the main components of martensite texture weakened until they completely decayed, while the intensities of some orientations increased in the texture of austenite (Fig. 3). In the annealing texture of austenite, the components with increased intensity appeared like the {112}<111>, {123}<111> orientation with some deviations. They showed the relation either of K-S or N-W with the components of the martensite texture formed at

deformation. The intensity of the {112}<111> orientation in the austenite texture, grew accompanied by simultaneous decrease of the ODF value for the {113}<110> orientation of the martensite, which according to the K-S relation, transformed into austenite {325}<233>, {112}<111> and {123}<111> orientation. Some components existing in the texture of the deformed and annealed austenite might be also described with a twin relation e.g. as the 60° rotation around the common <111> poles (Fig. 3).

4. Concluding remarks

The texture examination of two austenitic chromium-nickel steels, one of them stable X7CrNi24-11 and another metastable X10CrNi18-7, allowed the comparison of their behavior during deformation and annealing. The analysis also enabled to assess the influence of the $\gamma \rightarrow \alpha'$ phase transformation and the inverse $\alpha' \rightarrow \gamma$ one on the development of the both, deformation and annealing textures, respectively. The crystallographic relationships between the α' and γ phases could be thus also determine. Based on the results obtained the following conclusions were formulated:

1. The deformation textures of the austenitic steels, different in compositions and the phase stability could be described with the components of the austenite texture for the X7CrNi24-11 steel and the texture components of both the austenite and martensite for the X10CrNi18-7 steel.
2. In the process of deformation of the metastable steel the following phenomena took place: deformation of austenite, $\gamma \rightarrow \alpha'$ phase transformation and deformation of the previously formed martensite.
3. In the deformation textures of austenite of both examined steels, the major components included orientation from the α = <110>||ND fibre and the final deformation texture of austenite was close to the texture of the {110}<112>alloy-type characteristic for metals and alloys of low stacking fault energy (SFE).
4. The texture of martensite, which was formed during deformation, was close to the texture typical for the deformed ferrite with texture components of the <110>||RD type.
5. The annealing of the stable austenitic steel resulted in such changes of the austenite texture as disordering of texture, spreading of fibre α = <110>||ND, the appearance of new orientations {113}<332>, {326}<385>, and the formation of a weak fibre {340}<uvw>.
6. The reverse $\alpha' \rightarrow \gamma$ transformation of the martensite into austenite took place in the first stage of annealing of the metastable steel. Due to it, the texture of austenite got sharper at simultaneous weakening of that of martensite. The austenite which was formed upon annealing as a result of the inverse $\alpha' \rightarrow \gamma$ transformation preserved the deformation texture of the austenite, at the expense of which the martensite appeared. At lower temperatures of annealing the inverse transformation took place on the way of shearing and its products built a small volume fraction of the structure. At higher temperatures, the reaction proceeded in the diffusional manner. Above 750°C, a recrystallisation of both, the deformed austenite and the austenite formed during earlier stages of annealing due to the inverse $\alpha' \rightarrow \gamma$ transformation was observed.
7. The crystallographic relations between the orientations from the deformation and annealing textures of the austenite in the X7CrNi24-11 steel were best described by twinning relation i.e. the rotation by the (2n-1)x60° angle around selected <111> poles.
8. The Kurdjumov-Sachs (K-S) and Nishiyama-Wassermann (N-W) relations matched best the relationships of the austenite texture and that of martensite formed due to deformation as well as those between the orientations of the annealing texture of austenite and the deformation texture of martensite in the X10CrNi18-7 steel. Some orientations in the texture of the deformed and annealed austenite could also follow the twin relation.

Acknowledgements

The authors gratefully acknowledge the financial support from the Polish Committee of Scientific Research (KBN) under the contract No. 11.11.110.712.

REFERENCES

[1] J. Pospiech, J. Jura, A. Maciosowski, Transformation of Texture on the Example of the Bainitic Transformation, (International Conference on Texture of Materials) ICOTOM **3**, 235-241, France (1973).

[2] A. Maciosowski, S. Gorczyca, J. Pospiech, J. Jura, Structure, Texture and Mechanical Properties of the Product of Transformation of a Deformed Austenite in the 12H2NMB Steel, Arciwum Hutnictwa **234**, 2, 217-232 (1978).

[3] G. Brückner, J. Pospiech, Modelling and Verification of Texture Development During the $\alpha \rightarrow \gamma$ Phase Transformation in Steel, (International Conference on Texture of Materials) ICOTOM 11, 598-603 (1996).

[4] G. Brückner, J. Pospiech, I. Seidl, G. Gottstein, Orientation Correlation during Diffu-

sional $\alpha \rightarrow \gamma$ Phase Transformation in a Ferritic Low Carbon Steel, Scripta Materialia **44**, 2635-2640 (2001).

[5] G. Brückner, G. Gottstein, Transformation Texture during Diffusional $\alpha \rightarrow \gamma \rightarrow \alpha$ Phase Transformations in Ferritic Steels, ISIJ International **41**, 5, 159-172 (2001).

[6] G. J. Davies, J. S. Kalled, P. P. Morris, The Quantitative Prediction of Transformation Textures, Acta Metallurgica **24**, 159-172 (1976).

[7] D. Gododchild, W. T. Roberts, D. V. Wilson, Plastic Deformation and Phase Transformation in Textured Austenitic Stainless Steel, Acta Metallurgica **18**, 1137-1145 (1970).

[8] O. Hashimoto, S. Satoh, T. Tanaka, Formation of $\alpha \rightarrow \gamma \rightarrow \alpha$ Transformation Texture in Sheet Steel, Transactions ISIJ **23**, 1028-1037 (1983).

[9] Y. He, S. Godet, P. J. Jacques, J. J. Jonas, Crystallographic Relationships between FCC and BCC Crystals: A Study Using EBSD Techniques, Solid State Phenomena **105**, 121-126 (2005).

[10] B. Ravi Kumar, A. K. Singh, S. Das, D. K. Bhattacharya, Cold Rolling in AISI 304 Stainless Steel, Materials Science and Engineering **A364**, 132-139 (2004).

[11] A. L. Roytburd, Kurdjumov and his school in martensite of the 20th century; Materials Science and Engineering **A273-275**, 1-10 (1990).

[12] Y. H. Park, Z. H. Lee, The effect of nitrogen and heat treatment on the microstructure and tensile properties of 25 Cr-7Ni-1.5Mo-3W-xN duplex stainless steel castings, Materials Science and Engineering **A 297**, 78-84 (2001).

[13] A. F. Padilha, R. L. Plaut, P. R. Rios, Annealing of Cold-Worked Austenitic Stainless, ISIJ International **43**, 2, 135-143 (2003).

[14] J. C. Bavay, Les editions de physique, France (1993).

[15] D. Raabe, Texture and Microstructure Evolution During Cold Rolling of a Strip Cast and of Hot Rolled Austenitic Stainless Steel, Acta Materialia **45**, 3, 1137-1151 (1997).

[16] R. K. Ray, J. J. Jonas, Transformation Textures in Steel, International Materials Reviews **35**, 1, 1-36 (1990).

[17] K. Lücke, The Deformation of Recrystallization Textures in Metals and Alloys, (International Conference on Texture of Materials) ICOTOM 7, 195-210 Netherlands (1984).

[18] W. Ratuszek, Deformation and Recrystallisation Textures in Cu Based Alloys, in Polish, Rozprawy i Monografie AGH, 27, Kraków (1995).

[19] K. Sztwiertnia, Mechanizmy formowania się tekstur rekrystalizacji w metalach i stopach o sieci RSC, Instytut Metalurgii i Inżynierii Materiałowej PAN, Kraków (2001).

[20] K. Sztwiertnia, Orientation Aspect of the Recysstallization Nucleation in Highly Deformed Oily-crystalline Copper, Mater. Sci. Forum **99-104**, 467-470 (2004).

Received: 3 December 2007.